

The BTN3As B30.2/HMBPP Complex: New Insight into Phosphoantigen-Mediated Activation of a V γ 9V δ 2 T-Cell

The molecular mechanisms of phosphoantigens binding to BTN3A1 to activate a V γ 9V δ 2 T-cell has been elusive. Structural and biochemical analyses indicate that phosphoantigens bind to the intracellular domain of BTN3A1 to trigger an inside-out signal to activate V γ 9V δ 2 T-cells.

V γ 9V δ 2 T-cells play important roles in immune surveillance against pathogens and tumour cells. In a clinic, V γ 9V δ 2 T-cell-based therapy holds great potential for the treatment of a solid tumour. V γ 9V δ 2 T-cells can recognize non-peptide phosphoantigens (pAg) in a major histocompatibility complex (MHC)-independent manner. In the mid-1990s, isopentenyl pyro-

phosphate (IPP) and dimethylallyl pyrophosphate (DMAPP) were found to be immunostimulatory molecules of V γ 9V δ 2 T-cells. IPP and DMAPP are building blocks of the isoprenoid biosynthesis pathway that are widespread in prokaryotes and eukaryotes. These compounds might hence accumulate intracellularly during tumorigenesis and serve as self-antigens.¹ Later work showed

that (*E*)-1-hydroxy-2-methyl-but-2-enyl 4-diphosphate (HMBPP) is a more efficient activator of V γ 9V δ 2 T-cells. HMBPP is an intermediate in isoprenoid biosynthesis from bacteria and protozoa that use the non-mevalonate pathway (2-C-methyl-D-erythritol 4-phosphate [MEP]) for isoprenoid biosynthesis.² These molecules (IPP, DMAPP and HMBPP) are known as pAgs. The underlying molecu-

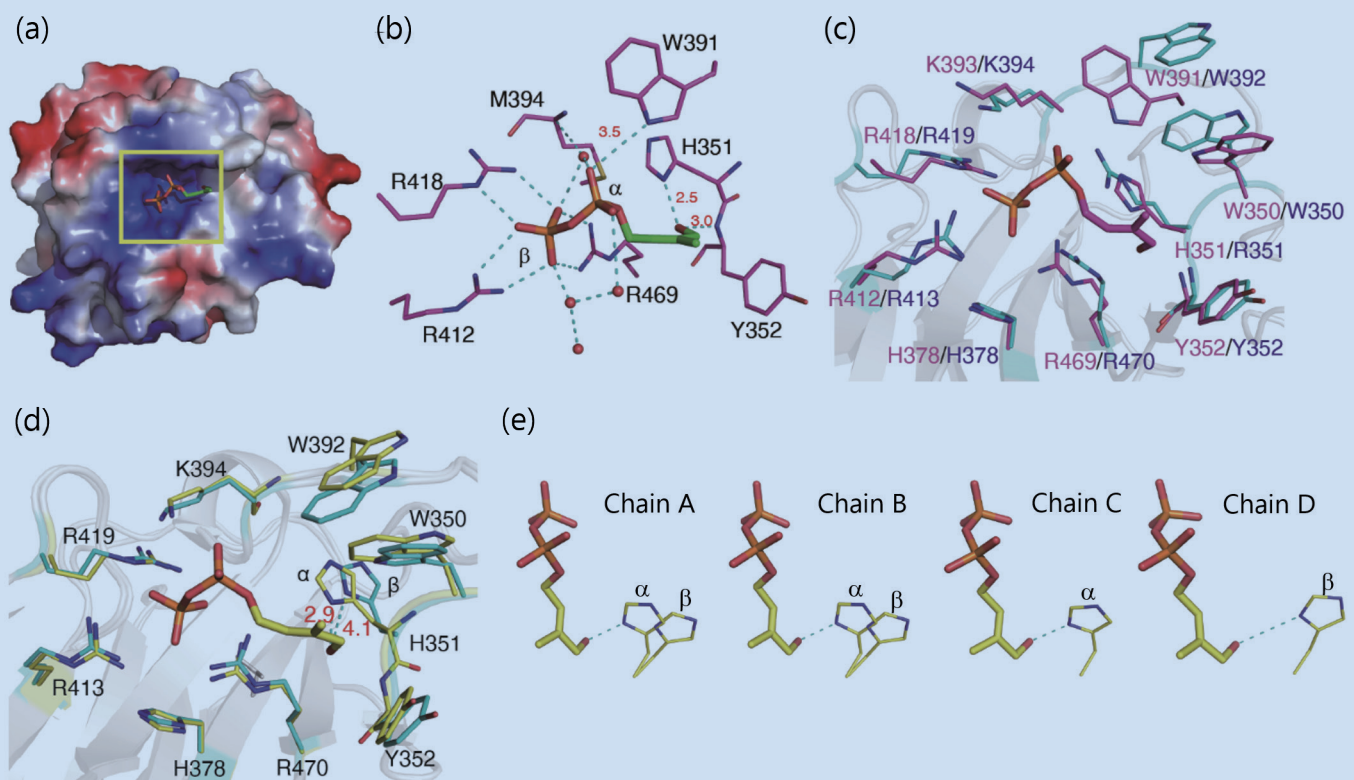


Fig. 1: (a) HMBPP bound to a basic pocket on the surface of the BTN3A1 B30.2 domain. (b) Interaction network of HMBPP with protein residues of interest; distances within 3.5 Å are shown as dashed lines. (c) Structural superimposition of the B30.2 domain of BTN3A1 (magenta) and BTN3A3 (blue). (d) Structural superimposition of the apo-form (blue) and HMBPP-bound BTN3A3 B30.2^{R351H} (yellow). (e) H351-HMBPP interactions in the BTN3A3 B30.2^{R351H} complex structure. The β , $\beta+\alpha$ and α conformers of H351 are seen in different chains of an asymmetric unit. [Reproduced from Ref. 5]

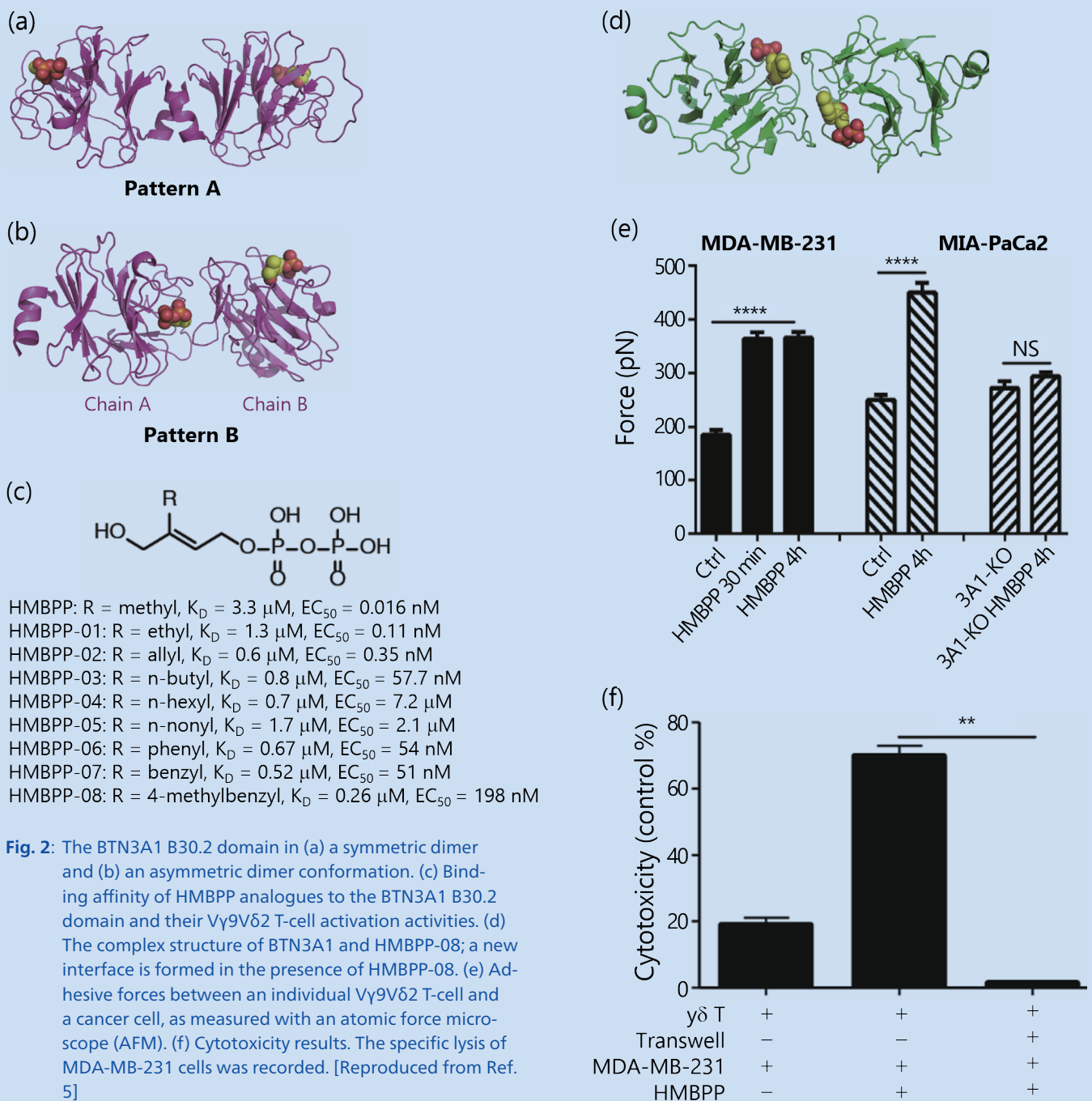
lar mechanism of pAg-mediated V γ 9V δ 2 T-cell activation is, however, unclear. In 2012, butyrophilin 3A1 (BTN3A1) was found to bind to pAg and to activate V γ 9V δ 2 T-cells.³

BTN3A1 belongs to the BTN3A family, which includes also BTN3A2 and BTN3A3 isoforms. BTN3A1 and BTN3A3 share a high sequence identity; both contain an intracellular B30.2 domain that is the putative pAg-binding site,

but the latter lacks a stimulatory activity towards V γ 9V δ 2 T-cells. Notably, substituting R351 with His enables the gain-of-function of BTN3A3 to bind to HMBPP.⁴ The molecular basis underlying the binding selectivity of BTN3As to pAg is unclear. To investigate the molecular mechanism and the binding selectivity, a research team led by Rey-Ting Guo (Chinese Academy of Sciences) solved the crystal structures of the cytoplasmic domain of BTN3A1

and BTN3A3 in apo-form and in a complex with HMBPP. All diffraction data sets were collected at **TPS 05A**, **TLS 13C1** and **TLS 15A1**.⁵

Figure 1(a) shows that HMBPP binds to a basic pocket formed on the surface of the BTN3A1 B30.2 domain. This pocket is constituted by the side chains of three arginine (R412, R418 and R469), one lysine (K393) and two histidine (H351 and H378) residues. These



residues form multiple hydrogen bond interactions to HMBPP (**Fig. 1(b)**). The distances between the 1-OH oxygen of HMBPP and H351 or Y352 were 2.5 and 3.0 Å respectively, indicating the presence of strong hydrogen bond interactions. The crystal structure of the BTN3A3 B30.2 domain was also solved to investigate the molecular mechanism underlying its lack of binding capacity to HMBPP. First, H351 that forms a hydrogen bond to 1-OH of HMBPP in BTN3A1 is Arg in BTN3A3 (**Fig. 1(c)**). This observation is supported by the gain-of-function of the R351H variant of BTN3A3. Second, the two conserved Trp residues W392 (W391 in 3A1) and W350 display different orientations in BTN3A3 and BTN3A1, so the hydrogen bond interactions between Pa and the loop region became diminished (**Fig. 1(c)**). H351 in apo-form BTN3A1 was also found to display varied conformations (**Fig. 1(d)**); the α -conformation is ready for HMBPP binding whereas the β -conformation is a loose form and distant from the hydrogen bond-forming position (**Fig. 1(d)**). In the HMBPP complex structure, H351 in three varied states is observed (**Fig. 1(e)**). These results indicate that the H351 might undergo conformational changes from the loose-form (β -conformation), intermediate ($\beta+\alpha$ conformation) to the bound-form (α -conformation) during the course of HMBPP binding.

BTN3A1 B30.2 could form a symmetric dimer or an asymmetric dimer in the crystal structure (**Figs. 2(a) and 2(b)**). AUC and FRET also enable the detection of the dimer formation of the BTN3A1 B30.2 domain. A chemical-probe approach (**Fig. 2(c)**) and structural data (structure of BTN3A1 B30.2 with HMBPP-08, **Fig. 2(d)**) supports involvement of an asymmetric dimer configuration in V γ 9V δ 2 T-cell activation. **Figure 2(e)** shows that the supplementation of HMBPP significantly enhances the interaction forces between BTN3A1 and the V γ 9V δ 2 T-cell receptor (TCR). Consistent with these results, the HMBPP-mediated MDA-MB-23 tumour cells killing by V γ 9V δ 2 T-cells requires direct cell-to-cell contact (**Fig. 2(f)**).

In summary, five conclusions have been drawn from the structural information and biochemical data. (1) The first structure of the complex of BTN3A1 B30.2 with HMBPP was obtained. (2) The antigen selectivity of BTN3A family members was investigated at the molecular level. (3) HMBPP binding to the intracellular B30.2 domain of BTN3A1 induced a conformational transition of H351. (4) An asymmetric dimer configuration was necessary for an efficient activation of the V γ 9V δ 2 T-cell. (5) HMBPP increased the avidity between the extracellular domain of BTN3A1 and V γ 9V δ 2 TCR, leading to an effective activation of the V γ 9V δ 2 T-cell. (Reported by Rey-Ting Guo, Chinese Academy of Sciences)

This report features the work of Yonghui Zhang, Rey-Ting Guo and their collaborators published in Immunity 50, 1043 (2019).

TPS 05A Protein Microcrystallography

TLS 13C1 SW60 – Protein Crystallography

TLS 15A1 Biopharmaceuticals Protein Crystallography

- Protein Crystallography
- Biological Macromolecules, Protein Structures, Life Science

References

1. Y. Tanaka, C. T. Morita, Y. Tanaka, E. Nieves, M. B. Brenner, B. R. Bloom, *Nature* **375**, 155 (1995).
2. M. Hintz, A. Reichenberg, B. Altincicek, U. Bahr, R. M. Gschwind, A. K. Kollas, E. Beck, J. Wiesner, M. Eberl, H. Jomaa, *FEBS Lett.* **509**, 317 (2001).
3. C. Harly, Y. Guillaume, S. Nedellec, C. M. Peigne, H. Monkkonen, J. Monkkonen, J. Li, J. Kuball, E. J. Adams, S. Netzer, J. Dechanet-Merville, A. Leger, T. Herrmann, R. Breathnach, D. Olive, M. Bonneville, E. Scotet, *Blood* **120**, 2269 (2012).
4. A. Sandstrom, C. M. Peigne, A. Leger, J. E. Crooks, F. Konczak, M. C. Gesnel, R. Breathnach, M. Bonneville, E. Scotet, E. J. Adams, *Immunity* **40**, 490 (2014).
5. Y. Yang, L. Li, L. Yuan, X. Zhou, J. Duan, H. Xiao, N. Cai, S. Han, X. Ma, W. Liu, C. C. Chen, L. Wang, X. Li, J. Chen, N. Kang, J. Chen, Z. Shen, S. R. Malwal, W. Liu, Y. Shi, E. Oldfield, R. T. Guo, Y. Zhang, *Immunity* **50**, 1043 (2019).